Design strategies for speed control of an inverter fed permanent magnet synchronous motor drive

Ramana Pilla*

Department of Electrical and Electronics Engineering,
GMR Institute of Technology,
Rajam, Andhra Pradesh, 532127, India
Email: pramana.gmrit@gmail.com
Email: ramana.pilla@gmrit.org
*Corresponding author

Alice Mary Karlapudy

Department of Electrical and Electronics Engineering,
Gudlavalleru Engineering College,
Gudlavalleru, Andhra Pradesh, 521356, India
Email: k.alicemary@gmail.com

Surya Kalavathi Munagala

Department of Electrical and Electronics Engineering,
JNTUH College of Engineering,
Hyderabad, Telangana, 500085, India
Email: munagala12@yahoo.co.in

Abstract: Permanent magnet synchronous motor (PMSM) drives are becoming more popular and replaces DC and Induction motor drives in industrial applications like rolling mills, home appliances, transport systems, robotics and factory automation, hybrid eclectic vehicles etc. Various control schemes are suggested in the literature for variable speed AC drives fed from static power sources. Among them field oriented control employing vector control strategies has become quite popular in recent years. A disadvantage of the scheme when applied to PMSM drives is that the motor always operates at a lagging power factor. In this paper, a generalised design strategy for speed control loop of an inverter fed PMSM drive is suggested. In this design for different combinations of currents, same torque can be generated, which leads to more general control scheme. The closed loop control system for PMSM drive is simulated using MATLAB. The performance figures of various cases such as internal p.f angle control, torque angle control and field oriented control can be obtained and verified through simulation for different power factors of the motor ranging from lagging to leading through unity.

Keywords: field oriented control; internal power factor angle control; permanent magnet synchronous motor; PMSM; PI controller; speed controller; torque angle control.

Reference to this paper should be made as follows: Pilla, R., Karlapudy, A.M. and Munagala, S.K. (2020) 'Design strategies for speed control of an inverter fed permanent magnet synchronous motor drive', *Int. J. Power and Energy Conversion*, Vol. 11, No. 1, pp.82–98.

Biographical notes: Ramana Pilla is an Associate Professor at the GMR Institute of Technology, Rajam, Andhra Pradesh, where he has been teaching for the past 17 years. He received his BTech in EEE, MTech in Electrical Power Engineering and PhD in EEE from the JNTUH, Hyderabad. He has published/presented 40 papers in international and national journals/conferences of repute. His areas of interest are control systems, power systems and electrical machine drives. He was a life member of ISTE, IE (India) and member of several academic bodies.

Alice Mary Karlapudy is a Professor at the Gudlavalleru Engineering College, Gudlavalleru, Andhra Pradesh, India. She received her BE in Electrical Power from the Mysore University and ME in Power Apparatus and Electric Drives from the IIT Roorkee, Uttar Pradesh. She obtained her PhD degree from the IIT Kharagpur, West Bengal. She has been teaching for the past 36 years, of which 25 years were devoted to her work in Government College of Engineering, Karnataka and 11 years in Andhra Pradesh. She has published more than 90 research papers of repute and guided three PhD scholars. A keen enthusiast of active research for 25 years, her areas of special interest include control system application to power electronics and electrical machine drives. She is a fellow member of the Institute of Engineers, India and Institute of Electronics and Tele Communication Engineers besides several academic bodies.

Surya Kalavathi Munagala is a Professor at the JNTUH College of Engineering Hyderabad, Telangana, where she has been teaching for the past 28 years. She received her BTech in EEE and ME in Power System Operation and Control from the Sri Venkateswara University, Tirupati, Andhra Pradesh. She received her PhD from the JNTUH Hyderabad and post-doctoral from the Carnegie Mellon University, Pittsburgh, USA. She has published more than 175 research papers of repute and guided 15 PhD scholars. Her areas of interest are high voltage engineering, control systems, power systems, power electronics and electrical machine drives. She is a professional member of IEEE, life member of ISTE and fellow member of the Institute of Engineers, India and member of several academic bodies.

1 Introduction

Permanent magnet synchronous motor (PMSM) is similar to salient pole synchronous motor, except that there is no field winding and the field is provided instead by mounting permanent magnets in the rotor. The elimination of field coil, DC supply and slip rings reduces the motor losses and complexity and hence improves the efficiency. These motors are widely used in AC servo drives because of their high torque to inertia ratio, high power density, high efficiency and power factor as compared to other conventional drive motors. Over the years different methods of closed loop control have been envisaged for improving the stability and dynamic response of the variable speed PMSM

drive (Pillay and Krishnan, 1988, 1989) fed from static devices either in open loop mode or short circuit mode involving stator voltage or current control (Diallo, 2004), torque angle control (Ramana et al., 2015a, 2016), power factor angle control (Ramana et al., 2015b) and field oriented control (FOC) (Ramana et al., 2015c).

Developments in the theory of controlling AC machines coupled with technological advances in power switching devices and converters along with control electronics now provide means for achieving controlled torque operation of AC machines. This is possible, if the armature and field currents can be independently controlled and spatial orthogonality can be maintained between the flux axis and mmf axis (Kron, 1930; Krishnan, 2001). If all the requirements are met at every instant of time, the torque will instantaneously follow the current and instantaneous torque control (R. Krishnan, 2001) will result. In AC machines, these requirements can be met only by external control. When driving a synchronous machine directly from the mains, the flux and torque will arise automatically in relation to the load (Clos, 2013), which leads to the variation of torque angle. The torque angle (δ) is defined as the angle between terminal voltage and excitation voltage and also called as load angle or power angle. The load leads to a modification of the torque angle until the steady state is reached. The transition occurs in the form of a periodic oscillation, which must be attenuated with damper windings. The variation of the torque angle complies with rotating the applied stator flux in relation to the rotor position without variation of the magnitude of the stator voltage. As long as the synchronous machine is in the stable region, the relation between torque angle and torque is proportional, so the torque angle can be utilised to control the torque. If the load on the motor increases, the rotor initially slows down, this increases torque angle. As a result the induced torque increases, speeding up the rotor up to the synchronous speed with a larger torque angle.

Normally, high dynamic response in AC motor is obtained by adopting FOC technique, in which the stator flux is aligned orthogonal to the rotor flux. In PMSM, FOC is realised by maintaining the direct-axis current equal to zero and controlling the quadrature-axis current as per the torque demand. For realising FOC (Blaschke, 1972), computations have to be carried out on-line for 3-phase to 2-phase and 2-phase to 3-phase coordinate transformation. This demands either a lot of computation time or complex hardware circuit. Also, the FOC results in a lagging power factor operation of the motor.

The internal power-factor (IPF) angle (angle between the field induced voltage and phase current) control (Muni et al., 1996) can be applied to PMSM for obtaining fast dynamic response. By maintaining the instantaneous IPF angle at zero degree, the PMSM can be made to give high dynamic performance similar to that obtainable from a separately excited DC motor. Thus, an IPF angle controlled drive can be used for applications demanding fast response.

Different types of control schemes have been suggested for variable speed AC drives (Wang, 2016; Kamel, 2009; Rudnicki, 2015) fed from static power converters. Among them direct and indirect vector control strategies have become quite popular in recent years. When applied these schemes to PMSM drives, there are certain drawbacks like instability, abrupt stopping etc. In this work, to overcome the above drawbacks, a generalised design strategy is suggested for speed control loop of an inverter fed PMSM drive.

The block diagram of proposed control system is shown in Figure 1, which consists of two loops namely the inner current loop and outer speed loop (Clos, 2013). In the outer loop, PI controller is used as speed controller to generate torque reference, T_e^*. From this

value, the reference values of currents i_{qs}^* and i_{ds}^* are computed for a desired internal angle (ψ) and torque angle (δ). This gives rise to the flexibility in choosing the p.f of the motor from lagging to leading through unity. The FOC (Ramana et al., 2015c) can also be obtained as a special case, by setting the power factor angle to be equal to the torque angle resulting in complete decoupling between the armature flux and field flux, thus producing a DC motor like behaviour. In this sense, the proposed control scheme is more general than conventional FOC. This paper is organised as follows: Firstly the mathematical model of PMSM is derived. Then the reference currents for desired ψ and δ are derived. Finally the simulation results are presented and discussed.

Figure 1 Block diagram representation of the proposed control scheme (see online version for colours)

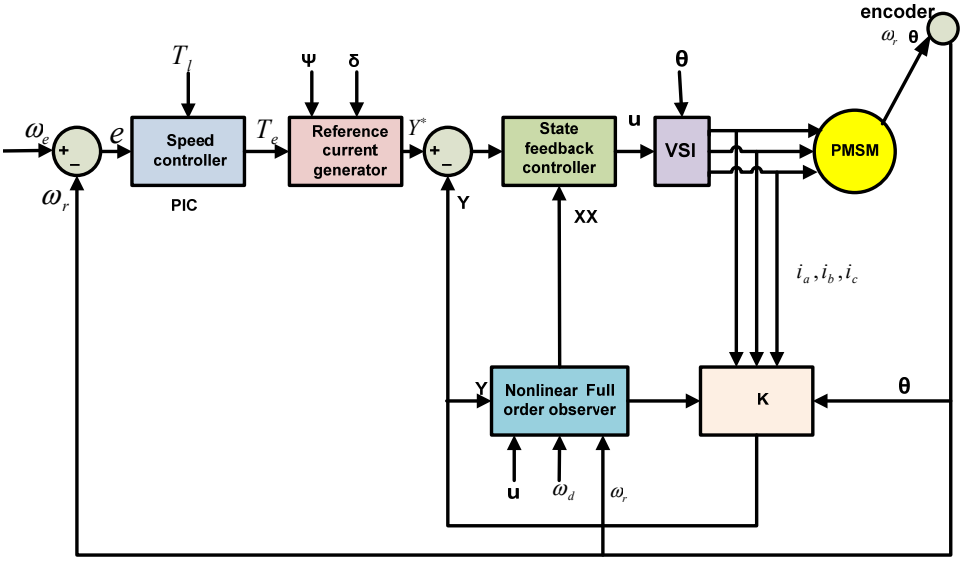

2 Mathematical model of PMSM

The schematic diagram of PMSM with damper windings is shown in Figure 2. The mathematical model of PMSM with damper winding has been developed on rotor reference (Kron, 1930) using Park's transformation.

The voltage equations for PMSM in rotor reference frame are

$$v_{qs} = r_a i_{qs} + l_{qs} p i_{qs} + l_{aq} p i_{qr} + \omega_r l_{ds} i_{ds} + \omega_r l_{ad} i_{dr} + \omega_r \Psi \tag{1}$$

$$v_{ds} = r_a i_{ds} + l_{ds} p i_{ds} + l_{ad} p i_{dr} - \omega_r l_{qs} i_{qs} - \omega_r l_{aq} i_{qr} \tag{2}$$

$$v_{qr} = r_{qr} i_{qr} + l_{qr} p i_{qr} + l_{aq} p i_{qs} \tag{3}$$

$$v_{dr} = r_{dr} i_{dr} + l_{dr} p i_{dr} + l_{ad} p i_{ds} \tag{4}$$

where $\Psi = l_{ad} i_{fr}$ = air gap flux linkage.

The electrical torque developed is

$$T_e = \frac{3}{2}\frac{P}{2}\left[\left(l_{ad} - l_{aq}\right) i_{qs} i_{ds} + l_{ad} i_{qs} i_{dr} - l_{aq} i_{qr} i_{ds} + \Psi i_{qs}\right] \tag{5}$$

The torque balance equation is

$$\frac{2}{P} Jp\omega_r = T_e - T_l - \frac{2}{P}\beta\omega_r \tag{6}$$

Hence, by using system and torque equations one can model PMSM.

Figure 2 Schematic diagram of PMSM with damper windings

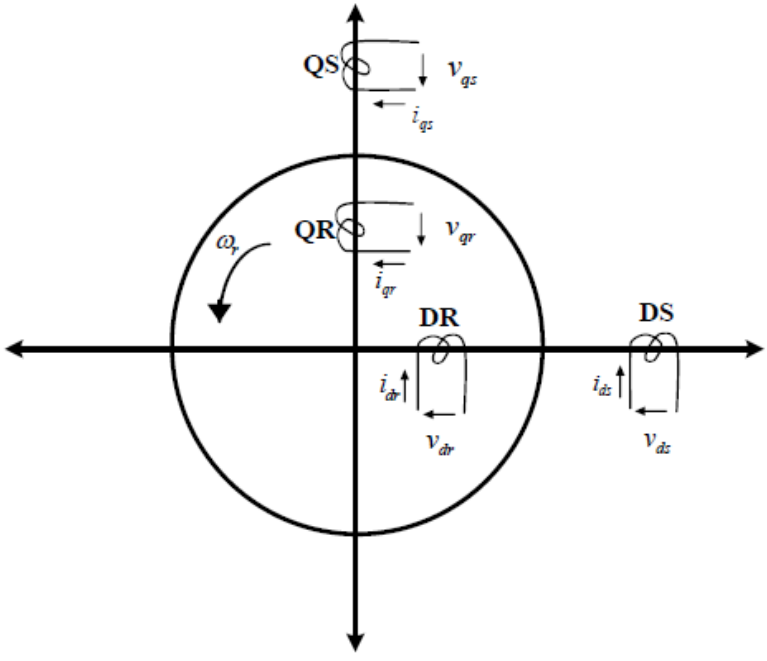

3 Design of the speed controller

In the conventional two-loop structure as shown in Figure 1, a proportional plus integral (PI) controller is used as a speed controller (Zhou and Wang, 2002) in the outer loop. The output of the PI controller is the reference torque T_e^*, from which the reference currents, i_{qs}^* and i_{ds}^* can be generated. The design of the gain constants of this controller is as follows:

The torque balance equation (6) for no. of poles, $P = 4$ is taken as

$$p\omega_r = \frac{2}{J}\left[T_e - T_l - \frac{\beta\omega_r}{2}\right] \tag{7}$$

The equation of PI controller is

$$T_e^* = k_p e + k_i \int_0^t e dt \tag{8}$$

where

$$e = (\omega_e - \omega_r) \tag{9}$$

Here ω_e is the set speed, ω_r is the reference speed and k_p and k_i are the proportional and integral gains of the PI controller respectively. Substituting equations (8) and (9) in equation (7) and taking Laplace transform,

$$(s\omega_r - \omega_{r0}) = \frac{2}{J}\left[\left(k_p + \frac{k_i}{s}\right)(\omega_e - \omega_r) - T_l - \left(\frac{\beta}{2}\right)\omega_r\right] \tag{10}$$

For $T_i = 0$ and $\omega_{r0} = \omega_e$ rearranging the terms in equation (10), from which the ratio, $\left(\frac{\omega_r}{\omega_e}\right)$ is obtained as

$$\frac{\omega_r}{\omega_e} = \frac{\frac{2}{J}\left(k_p + \frac{k_i}{s}\right)+1}{s + \frac{\beta}{J} + \frac{2}{J}\left(k_p + \frac{k_i}{s}\right)} = \frac{\left(\frac{2}{J}k_p + 1\right)s + \frac{2}{J}k_i}{s^2 + \left(\frac{\beta}{J} + \frac{2}{J}k_p\right)s + \frac{2}{J}k_i} \tag{11}$$

This is the standard form of transfer function for a second order system and the denominator can be represented in the form

$$s^2 + 2\zeta\omega_n s + \omega_n^2 = 0 \tag{12}$$

The characteristics of the above system is

$$s^2 + \left(\frac{\beta}{J} + \frac{2}{J}k_p\right)s + \frac{2}{J}k_i = 0 \tag{13}$$

On comparing the corresponding terms in equations (12) and (13), we have

$$\omega_n^2 = \frac{2k_i}{J} \tag{14}$$

$$2\zeta\omega_n = \frac{\beta}{J} + \frac{2k_p}{J} \tag{15}$$

From the above equations (14) and (15), the controller gains, k_i and k_p are obtained as,

$$k_i = \frac{J}{2}\omega_n^2 \tag{16}$$

$$k_p = J\zeta\omega_n - \frac{\beta}{2} \tag{17}$$

Assigning proper values of ζ and ω_n and using the values of J and β, the numerical values of k_i and k_p can be computed.

4 Determination of reference currents

The developed electrical torque given by equation (5) is a function of various states, i.e., the stator and rotor winding currents of the PMSM. Since, this function is a nonlinear one there are many possible combinations of these currents for the generation of same torque. Thus, there is a great deal of flexibility in the choice of reference values of these currents. The following three conditions are imposed to obtain unique solutions for these reference currents:

1 The internal angle is pre-specified to be ψ.

2 The torque angle is pre-specified to be δ.

3 All the reference currents should be real valued.

Figure 3 Phasor diagram

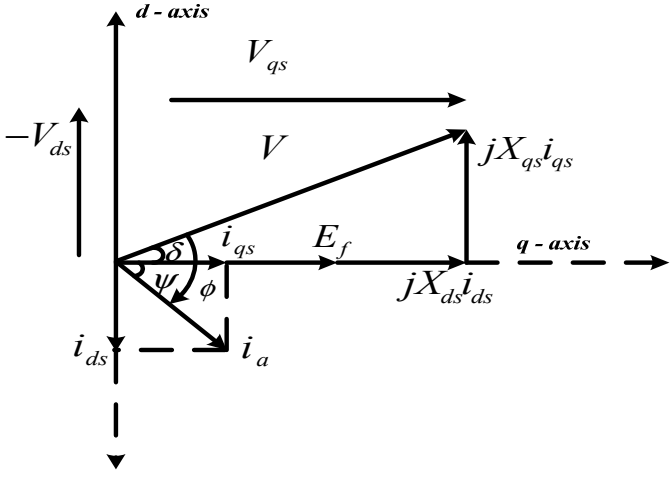

The Phasor diagram of a PMSM is as shown in figure 3. With a permanent magnet on the rotor, the motor has constant flux linkage, Ψ. Three sets of formulae for the reference currents are derived. One with specified δ, the second with specified ψ and the third for field oriented (FO) case.

4.1 Taking torque angle, δ as a specification

Referring to the Phasor diagram shown in Figure 3,

$$\tan\delta = \frac{-v_{ds}}{v_{qs}} \tag{18}$$

Substituting v_{qs} and v_{ds} from equations (1) and (2) in equation (18), will get

$$\tan\delta = \frac{-r_a i_{ds} - l_{ds} p i_{ds} - l_{ad} p i_{ds} + \omega_r l_{qs} i_{qs} + \omega_r i_{aq} i_{qr}}{r_a i_{qs} + l_{qs} p i_{qs} + l_{aq} p i_{qr} + \omega_r l_{ds} i_{ds} + \omega_r l_{ad} i_{dr} + \omega_r \Psi} \tag{19}$$

Under steady state condition with all p or $\frac{d}{dt}$ terms as well as i_{dr} and i_{qr} assumed to be zero. Then the above equation can be written as

$$\tan\delta = \frac{\omega_r l_{qs} i_{qs} - r_a i_{ds}}{r_a i_{qs} + \omega_r l_{ds} i_{ds} + \omega_r \Psi} \tag{20}$$

$$\left(r_a \tan\delta - \omega_r l_{qs}\right) i_{qs} = i_{ds}\left(-\omega_r l_{ds} \tan\delta - r_a\right) - \omega_r \Psi \tan\delta \tag{21}$$

Also the steady state torque from equation (5) for no. of poles, $P = 4$

$$T_e = 3\left[\left(l_{ad} - l_{aq}\right) i_{ds} i_{qs} + \Psi i_{qs}\right]$$

$$\therefore i_{qs} = \frac{T_e}{3\left[\left(l_{ad} - l_{aq}\right) i_{ds} + \Psi\right]} \tag{22}$$

From equations (21) and (22)

$$\left(r_a \tan\delta - \omega_r l_{qs}\right)\left[\frac{T_e}{3\left[\left(l_{ad} - l_{aq}\right) i_{ds} + \Psi\right]}\right] = i_{ds}\left(-\omega_r l_{ds} \tan\delta - r_a - \omega_r \Psi \tan\delta\right)$$

The simplification of above equation gives

$$i_{ds}^* = \frac{-q_2 \pm \sqrt{q_2^2 - 4 q_1 q_3}}{2 q_1}. \tag{23}$$

where

$$q_1 = 3\left(l_{ad} - l_{aq}\right)\left(-r_a - \omega_r l_{ds} \tan\delta\right)$$
$$q_2 = -3\left(l_{ad} - l_{aq}\right)\omega_r \Psi \tan\delta + 3\Psi\left(-r_a - \omega_r l_{ds} \tan\delta\right)$$
$$q_3 = -3\Psi^2 \omega_r \tan\delta - \left(r_a \tan\delta - \omega_r l_{qs}\right) T_e^*$$

and

$$i_{qs}^* = \frac{T_e^*}{3\left(l_{ad} - l_{aq}\right) i_{ds}^* + \Psi} \tag{24}$$

4.2 Taking internal angle, ψ as a specification

From the Phasor diagram shown in Figure 3

$$i_{ds} = i_{qs} \tan\psi \tag{25}$$

On substituting equation (25) in equation (22)

$$3\left(l_{ad} - l_{aq}\right) i_{qs}^2 \tan\psi + 3\Psi i_{qs} - T_e^* = 0 \tag{26}$$

The roots of the equation (26) can be obtained as

$$i_{qs}^{*} = \frac{-3\Psi \pm \sqrt{9\Psi^2 + 12T_e^{*}\left(l_{ad} - l_{aq}\right)\tan\psi}}{6\left(l_{ad} - l_{aq}\right)\tan\psi} \tag{27}$$

and

$$i_{ds}^{*} = i_{qs}^{*}\tan\psi \tag{28}$$

4.3 Field oriented control

In PMSM, FOC can be obtained by setting internal p.f. angle, ψ = 0 in equation (28). Therefore the reference current i_{ds}^{*} is given as

$$i_{ds}^{*} = 0 \tag{29}$$

From equations (22) and (29), reference current i_{qs}^{*} is obtained as,

$$i_{qs}^{*} = \frac{T_e^{*}}{3\Psi} \tag{30}$$

5 Design strategies for speed controller

The design methodology for the speed controller as outlined in the Section 3 allows one to choose ψ or δ or both of them independently in order to meet a certain control objective, such as unity power factor, field orientation etc. But, there is a scope for more general types of control, which can have useful engineering implications. In this section, the above design specifications are being viewed from this perspective.

A synchronous motor is a doubly excited machine (Kron, 1930; Krishnan, 2001) its armature winding is energised from an inverter and its field winding from a DC source. When synchronous motor is working at constant applied voltage, the resultant air gap flux as demanded by constant terminal voltage remains substantially constant. This resultant air gap flux is established by the co-operation of both AC in the armature winding and DC in the field winding. If the field current is sufficient enough to set up the air gap flux, as demanded by constant terminal voltage, V then magnetising current or lagging reactive volt ampere required from the AC source is zero and therefore, the motor operates at unity power factor. This field current which causes unity power factor operation of the synchronous motor is called normal excitation or normal field current.

If the field excitation E_f is made less than the normal excitation, i.e., the motor is under-excited then the deficiency in the flux (= constant air gap flux – flux setup by DC in the field winding) must be set-up by the armature winding. In order to do the needful, the armature winding draws a magnetising current or lagging reactive volt ampere from the AC source and as a result of it the motor operates at a lagging power factor. In case the field is made more than its normal excitation, i.e., the motor is over-excited, then the excess flux (= flux setup by DC in the field winding – resultant air gap flux) must be neutralised by the armature winding. The armature can do so only if it draws a demagnetising component of current from the AC source. Since in a motor, the

magnetising current lags the applied voltage by about 90°, the demagnetising component of current must lead the applied voltage by about 90°. In view of this, the excess flux can be counter balanced only if the armature takes a demagnetising current or leading reactive volt ampere from the AC source consequently the synchronous motor operates at a leading power factor.

6 Results and discussions

The PMSM with a constant flux corresponding to i_{fr} as 1A is considered. Then for different values of T_e, one can obtain the characteristics of i_{qs}, i_{ds}, armature current and power factor angle as a function of δ. From these characteristics, the r.m.s currents per phase as well as the power factor for given values of δ and T_e are compared, verified and validated through simulation results and finally it is observed that the wide range of practical working values of currents and the power factor for the stable performance of the motor.

For a motor the reactive power, Q is given by

$$Q = \frac{V}{X_s}\left(V - E_f \cos\delta\right) \tag{31}$$

From the Phasor diagram of Figure 3

$$\phi = \delta + \psi \tag{32}$$

Table 1 Performance figures for PMSM as a function of δ for variable T_e (D=design guidelines, S= simulation results)

Design specification δ	*Achieved values of*			
	ψ through	*ϕ through*		*cos ϕ*
Set value	*S*	*D*	*S*	*S*
3.8° (max. lag)	13.23	17	17.03	–0.25
8.04° (FOC) (lag case)	0.00	8.04	8.04	–0.18
8.23° (min. lag)	–6.63	1.56	1.59	–0.02
8.735° (upf value)	–8.734	0.03	0.03	1.0
8.74° (min. lead)	–8.75	–0.04	–0.01	0.99
35° (max. lead)	–58.63	–23.7	–23.62	0.06

Design specification δ	*Achieved values of*					
	i_{qs}		i_{ds}		i_{phase}	
Set value	*D*	*S*	*D*	*S*	*D*	*S*
3.8° (max. lag)	2.76	2.83	0.65	0.66	2.83	2.90
8.04° (FOC) (lag case)	2.82	3.23	0.00	0.00	2.82	3.23
8.23° (min. lag)	2.82	2.88	–0.33	–0.33	2.84	2.89
8.735° (upf value)	2.83	2.89	–0.43	–0.44	2.86	2.92
8.74° (min. lead)	2.83	2.89	–0.44	–0.44	2.86	2.92
35° (max. lead)	3.15	3.21	–5.17	–5.27	6.05	6.17

Figure 4 Family of characteristics of armature currents and power factor angle as a function of δ for different values of T_e (see online version for colours)

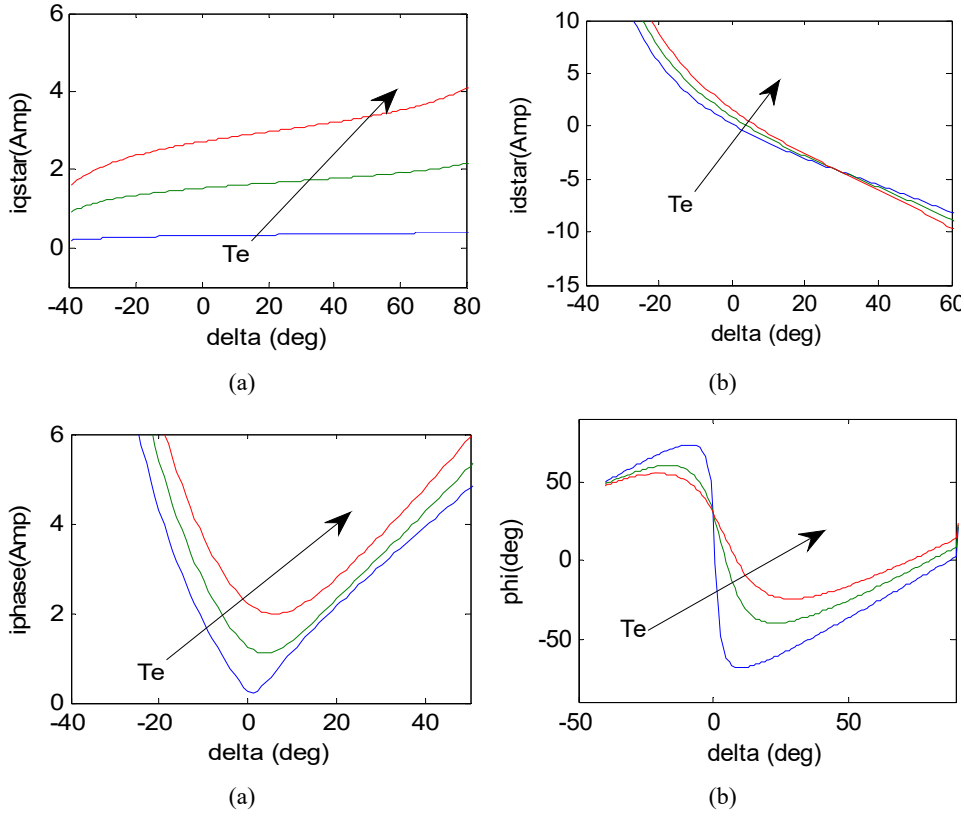

Table 2 Performance figures for PMSM as a function of δ with variable flux (only design values)

Range of δ for flux variable (–8° to 30°)	*Achieved values*				
	ϕ	$\cos\phi$	i_{qs}	i_{ds}	i_{phase}
–8° (max. lag)	48.00	–0.55	1.92	2.9	3.48
6.67° (FOC)	6.66	–0.95	2.1	0.0	2.1
8.1° (min. lag)	1.80	–0.24	2.1	–0.24	2.11
8.675° (upf)	0.0	1.00	2.1	–0.32	2.12
8.68° (min. lead)	–0.03	0.99	2.1	–0.32	2.12
30° (max. lead)	–24.7	0.90	2.3	–3.25	3.98

Figure 5 Family of characteristics of armature currents and p.f angle as a function of δ for different values of flux (see online version for colours)

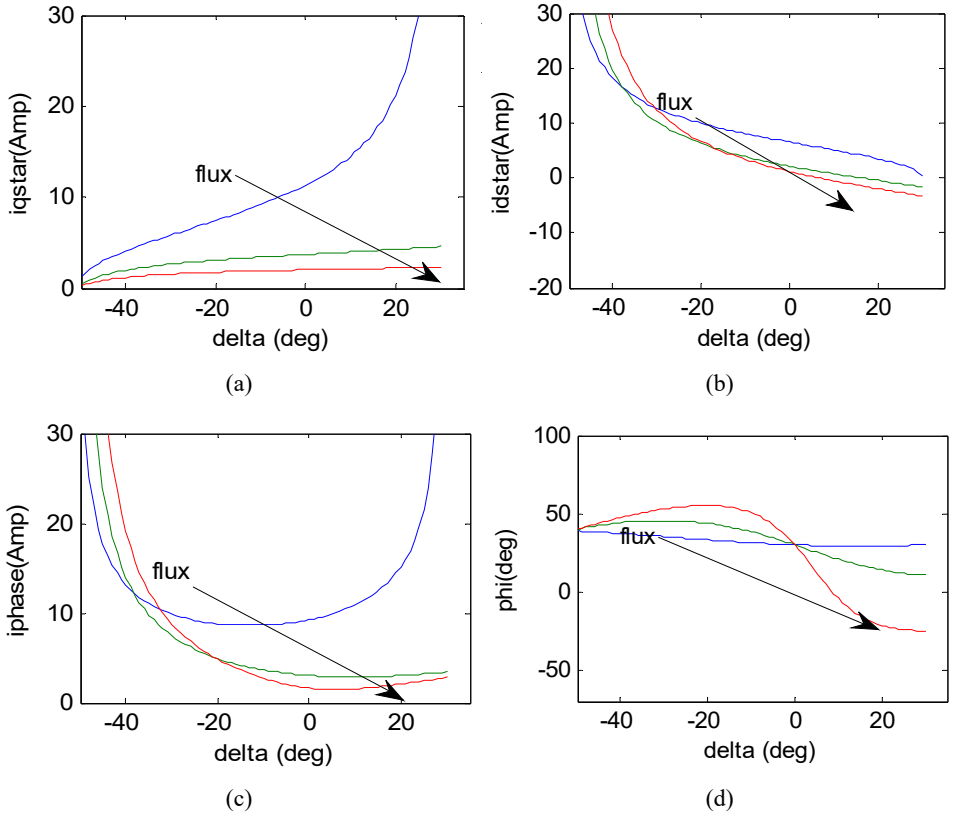

Figure 6 Family of characteristics of armature currents and p.f angle as a function of ψ for different values of T_e (see online version for colours)

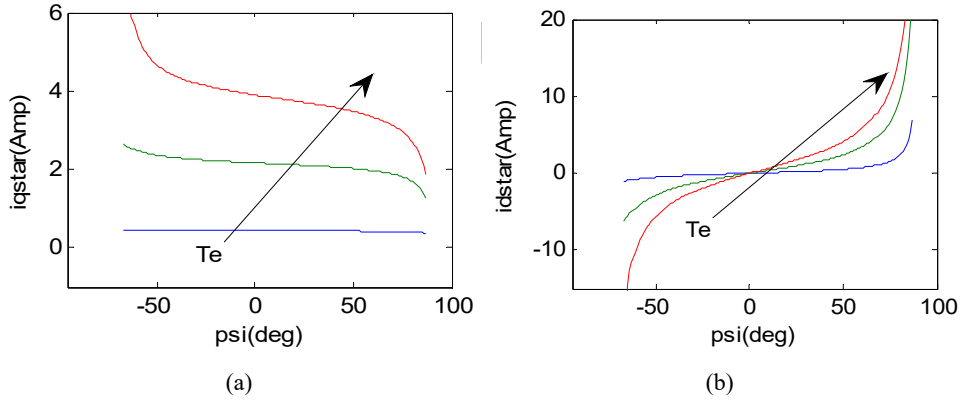

Figure 6 Family of characteristics of armature currents and p.f angle as a function of ψ for different values of T_e (continued) (see online version for colours)

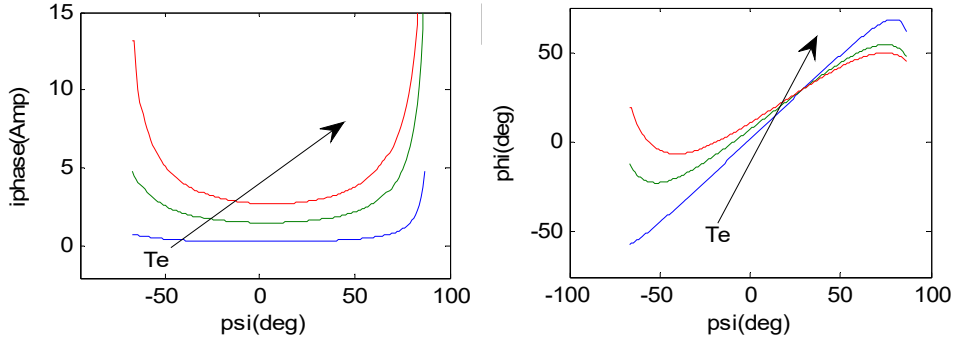

(c) (d)

Table 3 Performance figures for PMSM as a function of ψ for variable T_e (D = design guidelines, S = simulation results)

Design specification δ	*Achieved values of*			
	ψ through	*ϕ through*		*cos ϕ*
Set value	*S*	*D*	*S*	*S*
–49° (max lead)	44.06	–4.93	–4.92	0.22
–19.13° (min. lead)	19.17	–0.01	–0.01	0.99
–19.1° (upf)	19.15	0.00	0.00	1.0
–19° (min. lag)	19.05	0.05	0.05	0.99
0° (FOC)	10.79	11.00	10.79	–0.20
62° (max. lag)	–14.8	47.20	47.19	–0.99

Design specification δ	*Achieved values of*					
	i_{qs}		i_{ds}		i_{phase}	
Set value	*D*	*S*	*D*	*S*	*D*	*S*
–49° (max lead)	4.62	4.71	–5.3	–5.42	7.03	7.18
–19.13° (min. lead)	4.07	4.15	–1.41	–1.44	4.30	4.40
–19.1° (upf)	4.07	4.15	–1.41	–1.43	4.30	4.40
–19° (min. lag)	4.06	4.15	–1.4	–1.42	4.29	4.38
0° (FOC)	4.00	3.98	0.0	0.0	4.00	3.98
62° (max. lag)	3.30	3.37	6.20	6.33	7.02	7.17

Figure 7 Family of characteristics of armature currents and power factor for as a function of ψ for different values of flux (see online version for colours)

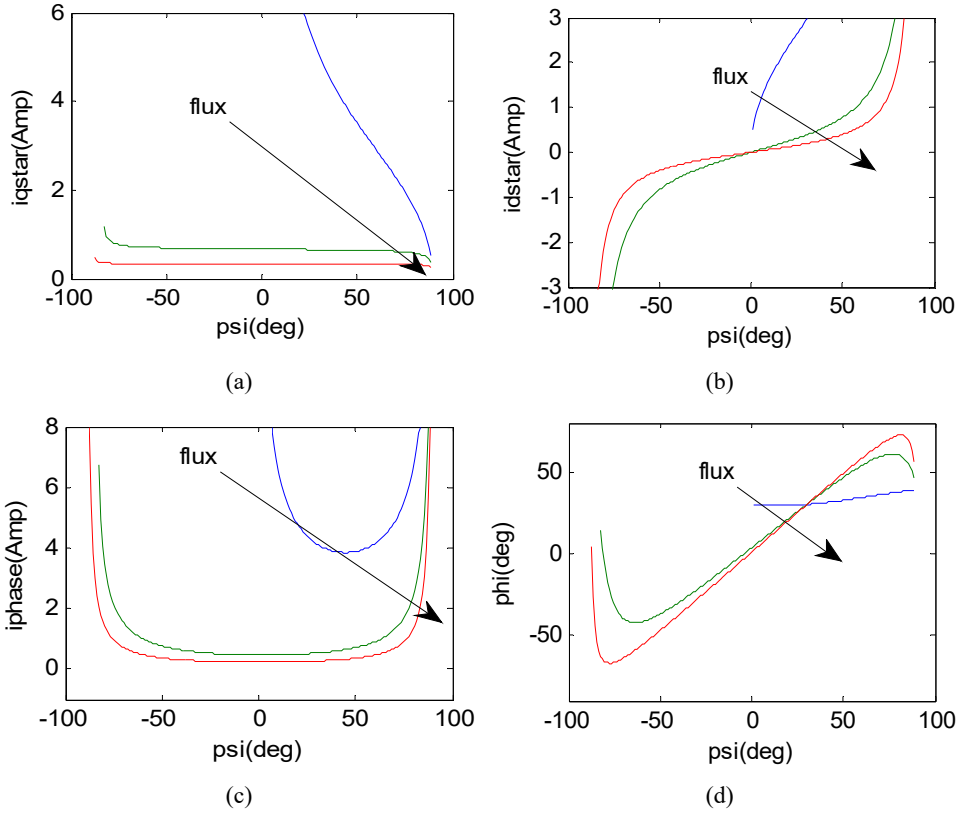

Table 4 Performance figures for PMSM as a function of ψ for variable flux only design values)

Range of ψ for flux variable (–22° to 80°)	*Achieved values of*				
	ϕ	$\cos\phi$	i_{qs}	i_{ds}	$i_{a,phase}$
–22° (max. lead)	–20.2	0.20	0.33	–0.13	0.36
–1.1° (min. lead)	–0.02	0.99	0.33	–0.006	0.33
–1.07° (upf)	0.0	1.0	0.33	–0.006	0.33
–1.03° (min. lag)	–0.22	0.99	0.33	–0.006	0.33
0.0° (FOC)	1.04	–0.5	0.33	0.0	0.33
80° (max lag)	72.3	–0.99	0.32	1.82	1.85

From the Figure 4 and Table 1, it is concluded that the u.p.f occurs at $\delta = 8.735°$ for the specification of δ with variable T_e. This point indicates $E_f\cos\delta = V$, i.e., normal excitation, under this condition $Q = 0$. For values of δ increasing from 3.8° to 8.735°, $\cos\delta$ decreases, therefore $E_f\cos\delta < V$. It depicts that the motor absorbing reactive power from the supply mains and is operating at a lagging p.f. At the same time ψ achieves positive value and p.f angle ϕ is also positive which is equal to 17° indicating a lagging p.f. The FOC ($\psi = 0°$), is achieved at $\delta = \phi = 8.04°$ and the p.f is –0.185 and is found to be always lagging. For values of δ decreasing from 35° to 8.735°, $\cos\delta$ increases. Therefore, $E_f\cos\delta > V$, indicates an over-excited condition, where the reactive power Q is negative, that means motor is delivering reactive power to the mains and hence works at leading p.f. Finally the working range of motor is restricted only from $\delta = 3.8°$ to 35° from the simulation even though the range of $\delta = 0°$ to 90° in design guidelines.

From Figure 5 and Table 2, it is concluded that the u.p.f occurs at $\delta = 8.675°$ for the specification of δ with variable flux. This point indicates $E_f\cos\delta = V$, i.e., normal excitation, under this condition $Q = 0$. For values of δ increasing from –8° to 8.675°, $\cos\delta$ decreases, therefore $E_f\cos\delta < V$. It depicts that the motor absorbing reactive power from the supply mains and is operating at a lagging p.f. The FOC ($\psi = 0°$), is achieved at $\delta = \phi = 6.67°$ and the p.f is –0.95 and is found to be always lagging. For values of δ decreasing from 30° to 8.67°, $\cos\delta$ increases. Therefore, $E_f\cos\delta > V$, indicates an over-excited condition, where the reactive power Q is negative, that means motor is delivering reactive power to the mains and hence works at leading p.f. Finally the working range of motor is restricted only from $\delta = –8°$ to 30° from the simulation even though the range of $\delta = 0°$ to 90° in design guidelines.

From Figure 6 and Table 3, it is concluded that the u.p.f occurs at $\psi = –19.1°$ for the specification of ψ with variable T_e. This point indicates $E_f\cos\delta = V$, i.e., normal excitation, under this condition $Q = 0$. For values of ψ increasing from –19.1° to 62°, $\cos\delta$ decreases, therefore $E_f\cos\delta < V$. It depicts that the motor absorbing reactive power from the supply mains and is operating at a lagging p.f. The FOC is achieved at $\psi = 0°$ and the p.f is –0.2 and is found to be always lagging. At this case $\delta = \phi = 10.79°$. For values of ψ decreasing from –49° to –19.1°, $\cos\delta$ increases. Therefore, $E_f\cos\delta > V$, indicates an over-excited condition, where the reactive power Q is negative, that means motor is delivering reactive power to the mains and hence works at leading p.f. Finally the working range of motor is restricted only from $\psi = –49°$ to 62° from the simulation even though the range is from $\psi = –49°$ to 90° in design guidelines.

From Figure 7 and Table 4, it is concluded that the u.p.f occurs at $\psi = –1.07°$ for the specification of ψ with variable T_e. This point indicates $E_f\cos\delta = V$, i.e., normal excitation, under this condition $Q = 0$. For values of ψ increasing from –1.07° to 80°, $\cos\delta$ decreases, therefore $E_f\cos\delta < V$. It depicts that the motor absorbing reactive power from the supply mains and is operating at a lagging p.f. The FOC is achieved at $\psi = 0°$ and the p.f is –0.5 and is found to be always lagging. At this case $\delta = \phi = 1.04°$ For values of ψ decreasing from –22° to –1.07°, $\cos\delta$ increases. Therefore, $E_f\cos\delta > V$, indicates an over-excited condition, where the reactive power Q is negative, that means motor is delivering reactive power to the mains and hence works at leading p.f. Finally the working range of motor is restricted only from $\psi = –22°$ to 80° from the simulation even though the range of $\psi = –49°$ to 90° in design guidelines.

7 Conclusions

Generalised approach of the design for torque angle and internal p.f angle control of a non-linear vector controlled PMSM drive is suggested and a wide range of dynamic performance is obtained by the variation of both δ and ψ. This also gives rise to the flexibility in choosing the p.f of the motor from lagging to leading (or vice versa) through unity. The special case of Field orientation control is also obtained by choosing torque angle such that the internal p.f angle made to be zero. This result in complete decoupling between the armature and field fluxes, allowing them to be controlled independently like a DC motor, improving the dynamic performance of the system. Design guidelines gives the clarity for the wider range of two angles, i.e., δ and ψ and hence ϕ. By these guidelines one can predict the physical implementation of the control system for its betterment.

References

Blaschke, F. (1972) 'The principle of field orientation as applied to the new TRANSVECTOR closed loop control system for rotating field machines', *Siemens Rev.*, Vol. 34, pp.217–220.

Clos, G. (2013) 'Torque angle control of the permanent magnet synchronous machine at the voltage margin', *15th European Conference on Power Electronics and Applications*, pp.1–9.

Diallo, G. (2004) 'A robust hybrid current control for permanent magnet synchronous motor drive', *IEEE Transactions on Energy Conversion*, Vol.19, No.1, pp.109–115.

Kamel, H.M., Hasanien, H.M. and Ibrahim, H.E.A (2009) 'Speed control of permanent magnet synchronous motor using fuzzy logic controller', *IEEE International Electric Machines and Drives Conference*, pp.1587–1591.

Krishnan, R. (2001) *Electric Motor Drives: Modeling, Analysis and Control*, 1st ed., Prentice Hall.

Kron, G. (1930) 'Generalized theory of electrical machinery', *Transactions of the American Institute of Electrical Engineers*, Vol. 49, No. 2, pp.666–683.

Muni, B.P., Pillai, S.K. and Saxena, S.N. (1996) 'A PC based internal power factor angle controlled interior permanent magnet synchronous motor drive', *27th Annual IEEE Power Electronics Specialists Conference*, pp.931–937.

Pillay, P. and Krishnan, R. (1988) 'Modeling of permanent magnet motor drives', *IEEE Transactions on Industrial Electronics*, Vol. 55, No. 4, pp.537–541.

Pillay, P. and Krishnan, R. (1989) 'Modeling, simulation and analysis of permanent magnet motor drives, Part I: the permanent magnet synchronous motor drive', *IEEE Transactions on Industry Applications*, Vol. 25, No. 2, pp.265273.

Ramana, P., Mary, K.A. and Kalavathi, S.M. (2016) 'Design methodology for torque-angle control of a non-linear vector controlled permanent magnet synchronous motor', *World Journal of Modelling Simulation*, Vol. 12, No. 4, pp.281–291.

Ramana, P., Mary, K.A., Kalavathi, S.M. and Kumar, V.G.D. (2015a) 'Design methodology for torque angle control of a non-linear vector controlled variable reluctance synchronous motor', *International Conference on Electrical, Electronics, Signals, Communication and Optimization*, pp.1–6.

Ramana, P., Mary, K.A., Kalavathi, S.M. and Avinash, A.P. (2015b) 'Design methodology for internal angle control of non-linear vector controlled variable reluctance synchronous motor', *International Journal of Applied Engineering Research*, Vol. 10, No. 1, pp.217–223.

Ramana, P., Mary, K.A., Kalavathi, S.M. and Kumar, V.G.D. (2015c) 'Design methodology for field orientation control of a non-linear vector controlled sinusoidal permanent magnet AC motor', *ARPN Journal Engineering and Technology*, Vol. 10, No. 5, pp.2159–2166.

Rudnicki, T., Czerwinski, R., Polok, D. and Sikora, A. (2015) 'Performance analysis of a PMSM drive with torque and speed control', *22nd International Conference Mixed Design of Integrated Circuits and Systems*, pp.562–566.

Wang, X., Ufnalski, B. and Grzesiak, L.M. (2016) 'Adaptive speed control in the PMSM drive for a non-stationary repetitive process using particle swarms', *10th International Conference on Compatibility, Power Electronics and Power Engineering*, pp.464–471.

Zhou, J. and Wang, Y. (2002) 'Adaptive back stepping speed controller design for a permanent magnet synchronous motor', *IEE Proceedings of Electric Power Applications*, Vol. 149, No. 2, pp.165–172.

Appendix

Table A1 Machine ratings and parameters

Motor specification	*Unit*	*Value*
Rated voltage	volt	400
Rated current	amp	2.17
Rated speed	rpm	1500
Number of poles	–	04
Rated power	kW	1.2
Power factor	–	0.8
Viscous coefficient	N.m/sec/rad	0.0048
Moment of Inertia	$kg.m^2$	0.048